



Ultrafast Mott transition driven by nonlinear electron-phonon interactionFrancesco Grandi ^{*}, Jiajun Li , and Martin Eckstein*Department of Physics, University of Erlangen-Nürnberg, 91058 Erlangen, Germany*

(Received 28 May 2020; revised 2 October 2020; accepted 11 January 2021; published 21 January 2021)

Nonlinear phononics holds the promise for controlling properties of quantum materials on the ultrashort timescale. Using nonequilibrium dynamical mean-field theory, we solve a model for the description of organic solids, where correlated electrons couple nonlinearly to a quantum phonon mode. Unlike previous works, we exactly diagonalize the local phonon mode within the noncrossing approximation to include the full phononic fluctuations. By exciting the local phonon in a broad range of frequencies near resonance with an ultrashort pulse, we show it is possible to induce a Mott insulator-to-metal phase transition. Conventional semiclassical and mean-field calculations, where the electron-phonon interaction decouples, underestimate the onset of the quasiparticle peak. This fact, together with the nonthermal character of the photoinduced metal, suggests a leading role of the phononic fluctuations and of the dynamic nature of the state in the vibrationally induced quasiparticle coherence.

DOI: [10.1103/PhysRevB.103.L041110](https://doi.org/10.1103/PhysRevB.103.L041110)**I. INTRODUCTION**

In the last decade, nonlinear phononics [1,2] has become one of the most promising pathways for the nonequilibrium control of quantum materials [3]. Within this approach, one can transiently stabilize a crystal structure unstable under equilibrium conditions by coherently exciting an infrared-active lattice mode which is nonlinearly coupled to a Raman-active phonon [4–10]. An analogous pathway suggests that the electronic properties of solids may be manipulated by the excitation of vibrational modes that couple nonlinearly with the local degrees of freedom of the electronic system [11–16].

Molecular solids provide a perfect playground for testing this mechanism [17,18]. A paradigm example is the charge-transfer (CT) salt ET-F₂TCNQ, which is an archetypical one-dimensional Mott insulator under equilibrium conditions and has been widely studied under photodoping [19,20]. Upon excitation of the molecular vibration $\omega_{\text{ph}} = 1000 \text{ cm}^{-1}$, the CT resonance at $\sim 5500 \text{ cm}^{-1}$ is redshifted, and an in-gap state at $2 \times \hbar\omega_{\text{ph}}$ appears [11,21]. Even more intriguing results have been obtained regarding light-induced superconductivity. The fulleride K₃C₆₀ [22] shows a superconducting state at temperatures almost ten times higher than the equilibrium T_c lasting a few picoseconds after excitation in the frequency range related to the T_{1u} mode of the C₆₀ molecule [23–25]. The organic superconductor $\kappa - (\text{BEDT} - \text{TTF})_2\text{Cu}[\text{N}(\text{CN})_2]\text{Br}$ (henceforth $\kappa - \text{Br}$) displays a similar behavior when the C = C stretching mode of the (BEDT – TTF)^{+0.5} molecule is excited [26]. Because the photoinduced superconducting response is correlated with the presence of an equilibrium coherent quasiparticle, it is an obvious relevant question, which will be analyzed in this Letter, whether nonlinear phononics can enhance quasiparticle

coherence in correlated electron systems. Moreover, we might ask if it is possible at all to replace the nonlinear phonons with some time dependent electronic Hamiltonian parameter. The rationale beyond this idea comes from a “natural” decoupling of the electron-phonon interaction. A typical local electron-phonon interaction gO_iX_i , where an electronic operator O_i couples to the displacement X_i of atom i , would give a term $F_i(t)O_i$ with a time dependent “force” $F_i(t) = g\langle X_i(t) \rangle$ in the electronic Hamiltonian when X_i is replaced by its time dependent expectation value in a coherent (macroscopically occupied) $\mathbf{q} = 0$ phonon state. For example, the experiments on ET-F₂TCNQ and $\kappa - \text{Br}$ were interpreted by an average shift and a periodic time dependence of the local Coulomb interaction (the Hubbard U) [11,26,27]. However, it is clear that the approximation $O_iX_i \approx O_i\langle X_i(t) \rangle$ is controlled by the fluctuations of the local displacement operator X_i relative to $\langle X_i(t) \rangle$, which are significant even when the phonons are globally in a macroscopic coherent mode. Even though the decoupling approach can successfully capture some experimental observations, it is, therefore, important to understand how quantum effects become manifest in nonlinear electron phononics [21].

In this Letter, we study a generalization of the Hubbard-Holstein model [28,29], which applies to ET-F₂TCNQ and $\kappa - \text{Br}$, with a quadratic coupling of a local displacement X_i to the doublon and the holon densities, so that, on average, X_i^2 modulates a local electron interaction U . The simulations indeed predict an insulator-to-metal transition (IMT), with a strong enhancement of the quasiparticle weight driven by the excitation of the local vibration. The vibrationally induced metallicity in the model cannot be accounted for by a decoupled Hamiltonian in which a time dependent U replaces the effect of the phonons, but instead the full quantum dynamics must be taken into account. We show that, even if the decoupled model takes into account the back-action of the electrons on the phonons (and vice versa), it cannot capture

^{*}Corresponding author: francesco.grandi@fau.de

phonon-related features in the electronic spectrum (Fano resonances) [30,31].

II. MODEL

We consider the generalized Hubbard-Holstein model, compactly written as

$$H(t) = H_{\text{el}} + H_{\text{el-ph}} + H_{\text{ph}} + H_{\text{driv}}(t) - \mu N. \quad (1)$$

The purely electronic part of the Hamiltonian is given by

$$H_{\text{el}} = -v_0 \sum_{(i,j),\sigma} (c_{i,\sigma}^\dagger c_{j,\sigma} + \text{H.c.}) + U \sum_i n_{i,\uparrow} n_{i,\downarrow}, \quad (2)$$

with nearest-neighbor hopping v_0 and local Hubbard interaction U ; μ is the chemical potential used to fix the occupation of each site to $\langle n_i \rangle = 1$. $v_0 = 1$ and \hbar/v_0 set the units for the energy and the times, respectively. The bare phonon Hamiltonian in Eq. (1) describes a band of Einstein phonons $H_{\text{ph}} = \omega_{\text{ph}} \sum_i (a_i^\dagger a_i + \frac{1}{2})$ where a_i^\dagger (a_i) is the creation (destruction) operator for a boson.

The electron-phonon interaction is given by [21]:

$$H_{\text{el-ph}} = 2 \sum_i (hH_i - dD_i) X_i^2, \quad (3)$$

where $H_i = (1 - n_{i,\uparrow})(1 - n_{i,\downarrow})$ ($D_i = n_{i,\uparrow} n_{i,\downarrow}$) are the holon (doublon) operators, and $X_i = \frac{a_i^\dagger + a_i}{\sqrt{2}}$ is the local displacement.

We take parameters $\omega_{\text{ph}} = 1.5$, so that we are far from the adiabatic regime, and assume the values $h = 0.1$ and $d = 0.35$ for the coupling constants. With this, the renormalized phonon frequencies on an isolated site occupied by a holon or doublon are $\omega_{\text{ph}}^h \sim 1.24 \omega_{\text{ph}}$ and $\omega_{\text{ph}}^d \sim 0.26 \omega_{\text{ph}}$, respectively. The renormalized frequency values obtained this way are in qualitative agreement with what is found for ET-F₂TCNQ, where a stiffening of the holon oscillator and a slackening of the doublon one is observed [21]. Note that $H_{\text{el-ph}}$ with $d \neq h$ breaks the particle-hole symmetry even on a bipartite lattice [32]. In experiments, the quadratic coupling of the phonon displacement and the electrons is confirmed by the $2\omega_{\text{ph}}$ feature in the optical absorption after phonon excitation [21]. The last term in Eq. (1) describes a linear coupling of the phonon displacement to an external electric field,

$$H_{\text{driv}}(t) = \sqrt{2}\omega_{\text{ph}} f(t) \sum_i X_i, \quad (4)$$

and we use a few-cycle excitation pulse $f(t)$ with different frequencies Ω (see Fig. 1 inset) to excite a coherent vibration of the phonon. Finally, we will compare the dynamics obtained from Eq. (1) with a decoupled Hamiltonian, in which the electron dynamics is determined by Eq. (2) with a time dependent interaction U :

$$H_{U\text{-driv}}(t) = H_{\text{el}}[U \rightarrow U(t)], \quad (5)$$

with different forms of $U(t)$ as described in the text.

We solve the time dependent models Eqs. (1) and (5) using nonequilibrium dynamical mean-field theory (NEDMFT) within noncrossing approximation (NCA) [33,34]. NCA has limitations in the description of the metallic phase of the Hubbard model at low temperatures and small U . Here, we apply it at high temperature and intermediate values of U ($U \sim$ bandwidth), where it is known to be qualitatively correct. NEDMFT maps the lattice problem into an

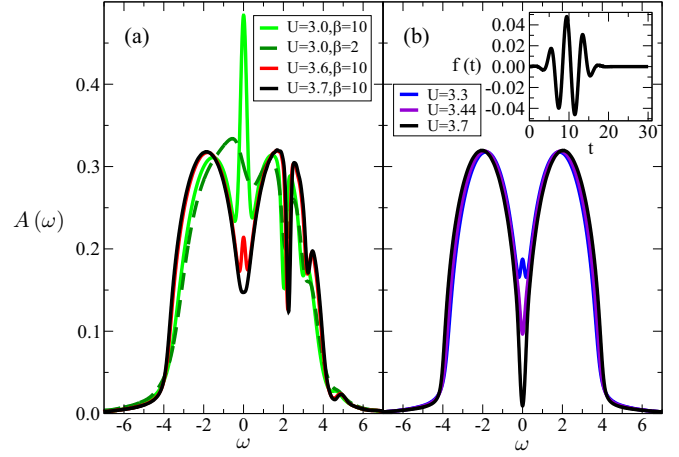


FIG. 1. (a) Equilibrium spectral functions $A(\omega)$ for the electron-phonon coupled system at several values of U and inverse temperature β . (b) Same for the Hubbard model without dynamic phonons, at $\beta = 10$. Inset: Time dependent driving field $f(t)$ [see Eq. (4)]. We keep the maximum amplitude (0.05) and the duration (20), while the frequency Ω is changed ($\Omega = 1.5$ in the plot, equal to ω_{ph}).

Anderson impurity model with a self-consistent hybridization function $\Delta(t, t')$. We use a semielliptic free density of states of width $4v_0$, leading to the closed form $\Delta(t, t') = v_0^2 G(t, t')$ in terms of the local contour-ordered electronic Green's function $G(t, t')$. For model (1), we include the full phonon Fock space and the nonlinear local electron-phonon dynamics exactly in the DMFT impurity model (similar to bosonic DMFT [35]) and take the cutoff in the phonon Hilbert space large enough ($N_{\text{ph}} = 18$ for mean occupations $|X_i| \lesssim 1$). This avoids potential ambiguities of alternative diagrammatic approaches for the local electron-phonon interaction [36–38]. Finally, energy dissipation of electrons to other degrees of freedom (phonons, spin fluctuations, etc.), which is fast in correlated insulators, is taken into account through a bosonic heat bath. The bath just adds a term to the hybridization [39,40], $\Delta(t, t') = v_0^2 G(t, t') + \Delta_{\text{Ohmic}}(t, t')$, where $\Delta_{\text{Ohmic}}(t, t') = \lambda G(t, t') D_{\text{Ohmic}}(t, t')$ is second order in the electron-boson coupling with temperature $1/\beta$ and Ohmic density of states [bath spectral density $J(\omega) = \sum_{\alpha} g_{\alpha}^2 \delta(\omega - \omega_{\alpha}) = \omega \theta(\omega_c - \omega)$, $\omega_c = 0.2$]. We take $\lambda = 0.242$, which is weak enough so that electronic spectra are not affected by the coupling to the bath.

III. RESULTS

In Fig. 1(a), we plot the electronic spectral function $A(\omega)$ of the model (1) for several values of the interaction U . At inverse temperature $\beta = 10$, shared by both the electronic and lattice subsystems, there is an IMT around $U = 3.6$, indicated by the appearance of a quasiparticle peak at $\omega \sim 0$. With increasing temperature, the quasiparticle peak vanishes, as the system crosses over into a bad metallic regime (see data for $U = 3.0$ and $\beta = 2$). The pronounced dip in the upper Hubbard band results from the hybridization between the doublon states and the phonon.

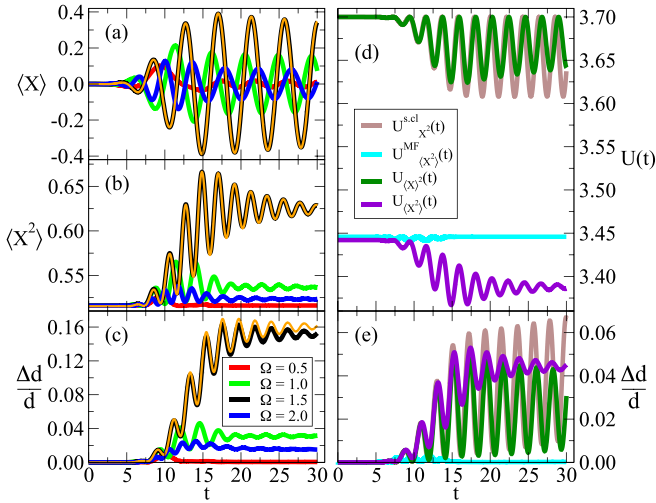


FIG. 2. Time evolution of the expectation value of the position operator $\langle X \rangle$ (a), its square $\langle X^2 \rangle$ (b), and the relative change of the double occupations with respect to the initial value $\frac{\Delta d}{d} = \frac{d(t) - d(0)}{d(0)}$ (c), at $U = 3.7$, $\beta = 10$, and field pulses $f(t)$ of different frequencies Ω . The thin orange lines represent the results at $\Omega = 1.5$ without Ohmic bath. (d) Time dependent $U_{X^2}^{\text{cl}}(t)$, $U_{X^2}^{\text{MF}}(t)$, $U_{\langle X \rangle^2}(t)$, and $U_{\langle X^2 \rangle}(t)$, as defined in Eq. (6). For the protocols $U_{\langle X \rangle^2}(t)$ and $U_{\langle X^2 \rangle}(t)$ the expectation values $\langle X(t) \rangle$ and $\langle X^2(t) \rangle$ correspond to the black line at $\Omega = 1.5$ of panels (a) and (b). (e) Time dependent $\frac{\Delta d}{d}$ as obtained from Eq. (5), with $U(t)$ shown in panel (d).

We now concentrate on parameters $U = 3.7$ and $\beta = 10$ above the IMT and attempt to induce the transition through phonon driving. The vibrational mode is pumped using a few-cycle pulse $f(t)$ as shown in the inset of Fig. 1, at different frequencies Ω . Figure 2 displays the resulting time evolution of several observables. While $\langle X \rangle$ oscillates around its equilibrium position $\langle X \rangle = 0$ with the bare phonon

frequency $\approx \omega_{\text{ph}}$ [Fig. 2(a)], $\langle X^2 \rangle$ oscillates around a shifted mean at a frequency $\approx 2\omega_{\text{ph}}$ [Fig. 2(b)]. The most pronounced response is observed at resonant pumping $\Omega = \omega_{\text{ph}} = 1.5$. At resonance, the double occupancy increases by about 15% compared to its initial value [Fig. 2(c)]. These changes go along with a photoinduced metallicity, as observed from the transient appearance of a quasiparticle peak at $\omega \sim 0$ in the time-resolved spectral function (Fig. 3, upper panels). The metallization survives the switch-off of the laser pulse up to the latest time ($t = 30$) of the simulation [Fig. 3(e)]. In addition to the quasiparticle peak, one observes oscillations at frequency $2\omega_{\text{ph}}$ in the spectrum, like in $\langle X^2 \rangle$. The broad range of frequencies Ω where we observe the onset of the peak at $\omega \sim 0$ verifies the genuine metallicity of the photoinduced state, with a small asymmetry around the observed maximum response (see Fig. 4).

We will now contrast these results with the decoupled model Eq. (5), where phonon variables in the electron-phonon interaction Eq. (3) are replaced by a classical field or the expectation value of a quantum operator, leading to a time dependent interaction. We compare four possible *Ansätze*: (i) X_i^2 is replaced by a classical field $X(t)^2$ self-consistently determined by the semiclassical equation of motion, (ii) a mean-field decoupling of the electron-phonon interaction Eq. (3) (of the kind $O_i X_i^2 \rightarrow \langle O_i \rangle X_i^2 + \langle X_i^2 \rangle O_i - \langle O_i \rangle \langle X_i^2 \rangle$) is performed while the full quantum dynamics of phonons is considered with the equation of motion for the density matrix, and X^2 is substituted with (iii) $\langle X(t) \rangle^2$ or (iv) $\langle X^2(t) \rangle$ obtained from the full DMFT calculation. Those approaches lead to

$$U \rightarrow \begin{cases} U - 2(d-h)X^2(t) \equiv U_{X^2}^{\text{cl}}(t) \\ U - 2(d-h)\langle X^2(t) \rangle \equiv U_{X^2}^{\text{MF}}(t) \\ U - 2(d-h)\langle X(t) \rangle^2 \equiv U_{\langle X \rangle^2}(t) \\ U - 2(d-h)\langle X^2(t) \rangle \equiv U_{\langle X^2 \rangle}(t) \end{cases}, \quad (6)$$

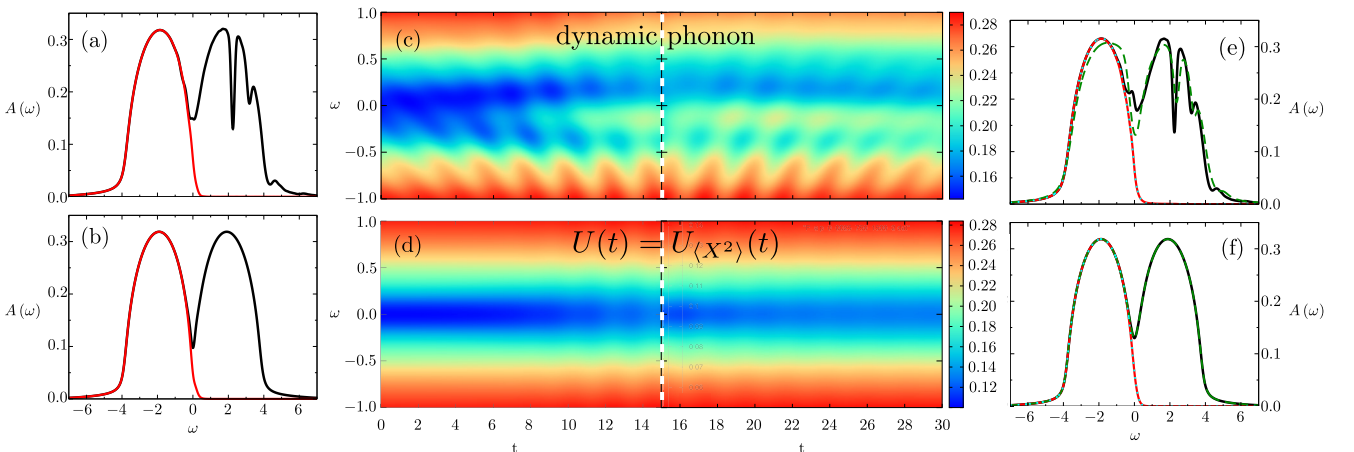


FIG. 3. Spectral functions for the dynamic phonon model at $U = 3.7$ (upper row) and the simplified approach $U(t) = U_{\langle X^2 \rangle}(t)$ (bottom row). Spectral function and occupation (black and red lines, respectively) at initial time $t = 0$ and at latest time $t = 30$ are shown in the left (a, b) and right columns (e–f), respectively. For intermediate time steps see Supplemental Material [41]. Additional lines in panels (e) and (f) show a fit $A^<(\omega, t) = A(\omega, t)/(1 + e^{\beta_{\text{eff}}\omega})$ to the occupation functions (dotted cyan lines), and the equilibrium spectral function (dashed green lines) for a system with the same total energy as the driven system at latest time $t = 30$ ($\beta \sim 2.083$ for the phonon case, $U \sim 3.388$, and $\beta = 10$ for the U -driven case). Middle panels (c, d): Time dependent spectral weight close to the Fermi level $\omega = 0$; spectral functions are obtained by forward Fourier transform $A(\omega, t) = -\frac{1}{\pi} \text{Im} \int ds G^R(t+s, t) e^{i\omega s}$ for $t < 15$ and by backward Fourier transform for $t > 15$ (dashed vertical line at $t = 15$).

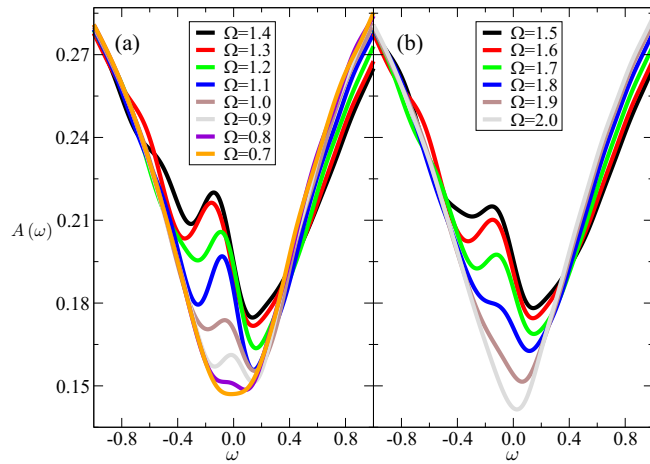


FIG. 4. Zoom around $\omega \sim 0$ of the time dependent (backward) spectral functions $A(\omega, t) = -\frac{1}{\pi} \text{Im} \int ds G^R(t, t-s) e^{i\omega s}$ at $t = 30$ after excitation pulses with frequency Ω below (a) and above (b) the bare phonon frequency ω_{ph} .

where we have assumed $\sum_i H_i = \sum_i D_i$ up to terms $\propto \hat{N}$. Figure 2(d) shows the resulting $U(t)$ for the almost-resonant driving case $\Omega = 1.5$. The two self-consistent protocols are computed using the driving term shown in the inset of Fig. 1. Clearly, for a general state of the quantum phonon, $\langle X \rangle^2 \neq \langle X^2 \rangle$. A time dependent function of the kind $U(t) = U + \Delta U [1 - \cos(2\omega_{\text{ph}} t)] \theta(t)$ can qualitatively describe the U driving guided by the classical X or by $\langle X \rangle$, while $U_{(X^2)}(t)$ looks more like an interaction quench. Finally, $U_{(X^2)}^{\text{MF}}(t)$, where the time dependent $\langle X^2(t) \rangle$ is computed using the density matrix, shows a tiny time dependence during the action of the external pulse only. Further details about the classical and mean-field dynamics are provided in Supplemental Material [41].

We note that $U_{(X^2)}^{\text{MF}}$ and $U_{(X^2)}$ deviate from U already in equilibrium, where the vacuum and thermal fluctuations of the phonon are responsible for a renormalization of U by ≈ -0.3 . In equilibrium, one finds that this renormalization rather accurately accounts for the shift of the IMT in the generalized Hubbard-Holstein model as compared to the standard Hubbard model. In Fig. 1(b), we show the equilibrium spectra of the Hubbard model at different U ; the IMT in the Hubbard-Holstein model Eq. (1) is indeed lowered by ≈ -0.3 compared to the static one. This quantitative agreement also shows that for the given parameters polaronic effects play a minor role in localizing the quasiparticles, at least under equilibrium conditions. In contrast to this observation, the nonequilibrium dynamics of quasiparticles and the vibrationally induced IMT in the model cannot be explained by a renormalized time dependent interaction. We compare in Fig. 3 the time dependent spectra $A(\omega, t)$ for the full dynamical phonons simulation and the $U_{(X^2)}$ driving protocol, that we take as representative of all the simplified protocols Eq. (6) [indeed, the qualitative dynamics of $A(\omega, t)$ is the same for all of them]. While we still notice some increase in the spectral weight at zero frequency, the quenchlike $U(t) =$

$U_{(X^2)}(t)$ (lower panels) does not reproduce the emergence of a zero-frequency peak. The rather different response of full DMFT treatment and the simplified approaches (6) is evident also in other observables: the relative change $\Delta d/d \sim 15\%$ in the double occupancy at resonant driving is almost three times larger than the change $\Delta d/d$ in the Hubbard model in response to the corresponding time dependent interactions [see Figs. 2(c) and 2(e)].

A possible explanation of the above findings is that the simplified approaches, which generally replace the phonon operators by semiclassical fields in the electronic problem, have underestimated the phonon-induced dissipation which favors metallization. However, we find that different electronic temperatures cannot explain our results. An effective temperature $1/\beta_{\text{eff}}$ obtained from a fit of the equilibrium fluctuation relation $A^<(\omega, t) = A(\omega, t)/(1 + e^{\beta_{\text{eff}}\omega})$ to the occupation functions $A^<(\omega, t)$ close to $\omega = 0$ at the latest simulation time yields an even lower effective temperature for the $U_{(X^2)}$ -driven case ($\beta_{\text{eff}} \sim 9.5$) compared to the full DMFT results ($\beta_{\text{eff}} \sim 6.2$); see continuous red lines and dotted cyan lines in Figs. 3(e) and 3(f). Moreover, $1/\beta_{\text{eff}}$ obtained in this way can only characterize the low-energy quasiparticles, while the total energy at $t = 30$ is that of a system at inverse temperature $\beta \sim 2.083$ [spectrum shown by the dashed green line in Fig. 3(e)], and $\langle X \rangle$ is still oscillating [Fig. 2(a)]. We, therefore, conclude that a time dependent interaction as in Eq. (6) plus electron cooling cannot faithfully describe the enhancement of metallicity in the photoexcited Mott insulator with nonlinear electron-phonon coupling. An analogous analysis shows that even for states closer to the metal-insulator transition the enhancement of metallicity is underestimated. A possible explanation is that in addition to the static renormalization of U through $\langle X^2 \rangle$ there is a dynamic contribution via virtual phonon emission and absorption. Such induced interactions go as g^2/ω_{ph} in the adiabatic phonon regime. In the presence of the X^2 nonlinearity, an oscillating phonon may act similar to a dynamically modulated electron-phonon coupling, which allows for interactions mediated via phonon-Floquet sidebands, with an energy denominator $1/(\omega_{\text{ph}} \pm \Omega)$. Thus, such interactions can be strongly renormalized, in particular close to resonance $\omega_{\text{ph}} = \Omega$. While the present parameter regime, close to the IMT and with not too well-separated energy scales between ω_{ph} and bandwidth, makes an analytic understanding difficult, the numerical results in Fig. 4 unambiguously demonstrate substantial enhancement of the quasiparticle peak around the resonance. Another effect could be driving-induced undressing of polarons [42–44], but as we have concluded above polaronic effects are probably not significant here.

IV. CONCLUSIONS

In this paper, we have analyzed a generalized Hubbard-Holstein model, relevant for the description of molecular solids, which is excited by an ultrafast pulse of local molecular vibration. By exactly treating the quantum phononic fluctuations, we show numerical evidence for the vibrationally induced emergence of a quasiparticle peak in the electronic

spectral function at $\omega \sim 0$, signaling the occurrence of an IMT. This observation should be relevant for the understanding of photoinduced superconductivity in molecular solids [26]. More generally, the striking difference of our results to a simplified treatment for the phonons implies the need for careful analysis of quantum phonon effects in the phononic control of electronic properties.

ACKNOWLEDGMENTS

F.G. would like to thank N. Dasari for the useful discussions about the Ohmic bath. We were supported by a European Research Council starting grant (Grant No. 716648). The authors gratefully acknowledge the computational resources and support provided by the Erlangen Regional Computing Center.

-
- [1] M. Först, C. Manzoni, S. Kaiser, Y. Tomioka, Y. Tokura, R. Merlin, and A. Cavalleri, Nonlinear phononics as an ultrafast route to lattice control, *Nat. Phys.* **7**, 854 (2011).
- [2] A. Subedi, A. Cavalleri, and A. Georges, Theory of nonlinear phononics for coherent light control of solids, *Phys. Rev. B* **89**, 220301(R) (2014).
- [3] D. N. Basov, R. D. Averitt, and D. Hsieh, Towards properties on demand in quantum materials, *Nat. Mater.* **16**, 1077 (2017).
- [4] M. Rini, R. Tobey, N. Dean, J. Itatani, Y. Tomioka, Y. Tokura, R. W. Schoenlein, and A. Cavalleri, Control of the electronic phase of a manganite by mode-selective vibrational excitation, *Nature (London)* **449**, 72 (2007).
- [5] A. D. Caviglia, R. Scherwitzl, P. Popovich, W. Hu, H. Bromberger, R. Singla, M. Mitrano, M. C. Hoffmann, S. Kaiser, P. Zubko, S. Gariglio, J.-M. Triscone, M. Först, and A. Cavalleri, Ultrafast Strain Engineering in Complex Oxide Heterostructures, *Phys. Rev. Lett.* **108**, 136801 (2012).
- [6] R. Mankowsky, A. Subedi, M. Först, S. O. Mariager, M. Chollet, H. T. Lemke, J. S. Robinson, J. M. Glowia, M. P. Miniti, A. Frano, M. Fechner, N. A. Spaldin, T. Loew, B. Keimer, A. Georges, and A. Cavalleri, Nonlinear lattice dynamics as a basis for enhanced superconductivity in $\text{YBa}_2\text{Cu}_3\text{O}_{6.5}$, *Nature (London)* **7529**, 71 (2014).
- [7] M. Först, R. I. Tobey, S. Wall, H. Bromberger, V. Khanna, A. L. Cavalieri, Y.-D. Chuang, W. S. Lee, R. Moore, W. F. Schlotter, J. J. Turner, O. Krupin, M. Trigo, H. Zheng, J. F. Mitchell, S. S. Dhesi, J. P. Hill, and A. Cavalleri, Driving magnetic order in a manganite by ultrafast lattice excitation, *Phys. Rev. B* **84**, 241104(R) (2011).
- [8] M. Först, A. D. Caviglia, R. Scherwitzl, R. Mankowsky, P. Zubko, V. Khanna, H. Bromberger, S. B. Wilkins, Y.-D. Chuang, W. S. Lee, W. F. Schlotter, J. J. Turner, G. L. Dakovski, M. P. Miniti, J. Robinson, S. R. Clark, D. Jaksch, J.-M. Triscone, J. P. Hill, S. S. Dhesi, and A. Cavalleri, Spatially resolved ultrafast magnetic dynamics initiated at a complex oxide heterointerface, *Nat. Mater.* **14**, 883 (2015).
- [9] T. F. Nova, A. Cartella, A. Cantaluppi, M. Först, D. Bossini, R. V. Mikhaylovskiy, A. V. Kimel, R. Merlin, and A. Cavalleri, An effective magnetic field from optically driven phonons, *Nat. Phys.* **2**, 132 (2017).
- [10] E. Pomarico, M. Mitrano, H. Bromberger, M. A. Sentef, A. Al-Temimy, C. Coletti, A. Stöhr, S. Link, U. Starke, C. Cacho, R. Chapman, E. Springate, A. Cavalleri, and I. Gierz, Enhanced electron-phonon coupling in graphene with periodically distorted lattice, *Phys. Rev. B* **95**, 024304 (2017).
- [11] R. Singla, G. Cotugno, S. Kaiser, M. Först, M. Mitrano, H. Y. Liu, A. Cartella, C. Manzoni, H. Okamoto, T. Hasegawa, S. R. Clark, D. Jaksch, and A. Cavalleri, THz-Frequency Modulation of the Hubbard U in an Organic Mott Insulator, *Phys. Rev. Lett.* **115**, 187401 (2015).
- [12] D. M. Kennes, E. Y. Wilner, D. R. Reichman, and A. J. Millis, Transient superconductivity from electronic squeezing of optically pumped phonons, *Nat. Phys.* **13**, 479 (2017).
- [13] M. A. Sentef, Light-enhanced electron-phonon coupling from nonlinear electron-phonon coupling, *Phys. Rev. B* **95**, 205111 (2017).
- [14] A. Marciniak, S. Marcantoni, F. Giusti, F. Glerean, G. Sparapassi, T. Nova, A. Cartella, S. Latini, F. Valiera, A. Rubio, J. van den Brink, F. Benatti, and D. Fausti, Vibrational coherent control of localized d-d electronic excitation, *Nat. Phys.* (2021), doi: 10.1038/s41567-020-01098-8.
- [15] M. Puviani and M. A. Sentef, Quantum nonlinear phononics route towards nonequilibrium materials engineering: Melting dynamics of a ferroelectric charge density wave, *Phys. Rev. B* **98**, 165138 (2018).
- [16] A. Klein, M. H. Christensen, and R. M. Fernandes, Laser-induced control of an electronic nematic quantum phase transition, *Phys. Rev. Research* **2**, 013336 (2020).
- [17] M. Lang and J. Müller, Organic superconductors, in *The Physics of Superconductors: Vol. II. Superconductivity in Nanostructures, High-Tc and Novel Superconductors, Organic Superconductors*, edited by K. H. Bennemann and J. B. Ketterson (Springer-Verlag, Berlin, 2004), pp. 453–554.
- [18] A. Ardavan, S. Brown, S. Kagoshima, K. Kanoda, K. Kuroki, H. Mori, M. Ogata, S. Uji, and J. Wosnitza, Recent topics of organic superconductors, *J. Phys. Soc. Jpn.* **81**, 011004 (2012).
- [19] H. Okamoto, H. Matsuzaki, T. Wakabayashi, Y. Takahashi, and T. Hasegawa, Photoinduced Metallic State Mediated by Spin-Charge Separation in a One-Dimensional Organic Mott Insulator, *Phys. Rev. Lett.* **98**, 037401 (2007).
- [20] M. Mitrano, G. Cotugno, S. R. Clark, R. Singla, S. Kaiser, J. Stähler, R. Beyer, M. Dressel, L. Baldassarre, D. Nicoletti, A. Perucchi, T. Hasegawa, H. Okamoto, D. Jaksch, and A. Cavalleri, Pressure-Dependent Relaxation in the Photoexcited Mott Insulator $\text{ET-F}_2\text{TCNQ}$: Influence of Hopping and Correlations on Quasiparticle Recombination Rates, *Phys. Rev. Lett.* **112**, 117801 (2014).
- [21] S. Kaiser, S. R. Clark, D. Nicoletti, G. Cotugno, R. I. Tobey, N. Dean, S. Lupi, H. Okamoto, T. Hasegawa, D. Jaksch, and A. Cavalleri, Optical properties of a vibrationally modulated solid state Mott insulator, *Sci. Rep.* **4**, 3823 (2014).
- [22] M. Capone, M. Fabrizio, C. Castellani, and E. Tosatti, Colloquium: Modeling the unconventional superconducting properties of expanded A_3C_{60} fullerides, *Rev. Mod. Phys.* **81**, 943 (2009).
- [23] M. Mitrano, A. Cantaluppi, D. Nicoletti, S. Kaiser, A. Perucchi, S. Lupi, P. Di Pietro, D. Pontiroli, M. Riccò, S. R. Clark,

- D. Jaksch, and A. Cavalleri, Possible light-induced superconductivity in K_3C_{60} at high temperature, *Nature (London)* **7591**, 461 (2016).
- [24] A. Cantaluppi, M. Buzzi, G. Jotzu, D. Nicoletti, M. Mitrano, D. Pontiroli, M. Riccò, A. Perucchi, P. Di Pietro, and A. Cavalleri, Pressure tuning of light-induced superconductivity in K_3C_{60} , *Nat. Phys.* **8**, 837 (2018).
- [25] M. Budden, T. Gebert, M. Buzzi, G. Jotzu, E. Wang, T. Matsuyama, G. Meier, Y. Laplace, D. Pontiroli, M. Riccò, F. Schlawin, D. Jaksch, and A. Cavalleri, Evidence for metastable photo-induced superconductivity in K_3C_{60} , [arXiv:2002.12835](https://arxiv.org/abs/2002.12835).
- [26] M. Buzzi, D. Nicoletti, M. Fechner, N. Tancogne-Dejean, M. A. Sentef, A. Georges, T. Biesner, E. Uykur, M. Dressel, A. Henderson, T. Siegrist, J. A. Schlueter, K. Miyagawa, K. Kanoda, M.-S. Nam, A. Ardavan, J. Coulthard, J. Tindall, F. Schlawin, D. Jaksch, and A. Cavalleri, Photomolecular High-Temperature Superconductivity, *Phys. Rev. X* **10**, 031028 (2020).
- [27] Y. Kawakami, S. Iwai, T. Fukatsu, M. Miura, N. Yoneyama, T. Sasaki, and N. Kobayashi, Optical Modulation of Effective On-Site Coulomb Energy for the Mott Transition in an Organic Dimer Insulator, *Phys. Rev. Lett.* **103**, 066403 (2009).
- [28] P. Pincus, Polaron effects in the nearly atomic limit of the Hubbard model, *Solid State Commun.* **11**, 51 (1972).
- [29] J. E. Hirsch, Dynamic Hubbard Model, *Phys. Rev. Lett.* **87**, 206402 (2001).
- [30] K. Itoh, H. Itoh, M. Naka, S. Saito, I. Hosako, N. Yoneyama, S. Ishihara, T. Sasaki, and S. Iwai, Collective Excitation of an Electric Dipole on a Molecular Dimer in an Organic Dimer-Mott Insulator, *Phys. Rev. Lett.* **110**, 106401 (2013).
- [31] D. Neuhauser, Tae-Jun Park, and J. I. Zink, Analytical Derivation of Interference Dips in Molecular Absorption Spectra: Molecular Properties and Relationships to Fano's Antiresonance, *Phys. Rev. Lett.* **85**, 5304 (2000).
- [32] J. E. Hirsch, Electron-hole asymmetry is the key to superconductivity, *Int. J. Mod. Phys. B* **17**, 3236 (2003).
- [33] H. Aoki, N. Tsuji, M. Eckstein, M. Kollar, T. Oka, and P. Werner, Nonequilibrium dynamical mean-field theory and its applications, *Rev. Mod. Phys.* **86**, 779 (2014).
- [34] M. Eckstein and P. Werner, Nonequilibrium dynamical mean-field calculations based on the noncrossing approximation and its generalizations, *Phys. Rev. B* **82**, 115115 (2010).
- [35] H. U. R. Strand, M. Eckstein, and P. Werner, Nonequilibrium Dynamical Mean-Field Theory for Bosonic Lattice Models, *Phys. Rev. X* **5**, 011038 (2015).
- [36] P. Werner and M. Eckstein, Phonon-enhanced relaxation and excitation in the Holstein-Hubbard model, *Phys. Rev. B* **88**, 165108 (2013).
- [37] P. Werner and M. Eckstein, Effective doublon and hole temperatures in the photo-doped dynamic Hubbard model, *Structural Dynamics* **3**, 023603 (2016).
- [38] Hsing-Ta Chen, G. Cohen, A. J. Millis, and D. R. Reichman, Anderson-Holstein model in two flavors of the noncrossing approximation, *Phys. Rev. B* **93**, 174309 (2016).
- [39] M. Eckstein and P. Werner, Photoinduced States in a Mott Insulator, *Phys. Rev. Lett.* **110**, 126401 (2013).
- [40] F. Peronaci, O. Parcollet, and M. Schiró, Enhancement of local pairing correlations in periodically driven Mott insulators, *Phys. Rev. B* **101**, 161101(R) (2020).
- [41] See Supplemental Material at <http://link.aps.org/supplemental/10.1103/PhysRevB.103.L041110> for additional data showing the spectral functions and occupations at intermediate time steps for the two excitation protocols illustrated in Fig. 3 of the Letter, as well as some technical details about the semiclassical and mean-field treatments of the electron-phonon interaction.
- [42] J. E. Hirsch, Quasiparticle undressing in a dynamic Hubbard model: Exact diagonalization study, *Phys. Rev. B* **66**, 064507 (2002).
- [43] J. E. Hirsch, Polaronic superconductivity in the absence of electron-hole symmetry, *Phys. Rev. B* **47**, 5351 (1993).
- [44] P. Gaal, W. Kuehn, K. Reimann, M. Woerner, T. Elsaesser, and R. Hey, Internal motions of a quasiparticle governing its ultrafast nonlinear response, *Nature (London)* **450**, 1210 (2007).